RevMexAA (Serie de Conferencias), **30**, 90–95 (2007)

EVIDENCE FOR PRE-SN MASS LOSS IN THE GALACTIC SNR 3C 58

Gwen C. Rudie[1] and Robert A. Fesen[1]

RESUMEN

Discutimos los hallazgos de la emisión óptica asociada al remanente de supernova 3C 58 (Fesen et al. 2007) mediante un reconocimiento de imagen y espectroscópico, y lo relacionamos con la pérdida de masa de pre-supernova. Las velocidades radiales espectroscópicas de más de 450 nudos de emisión dentro del remanente muestran dos distintas poblaciones cinemáticas: un grupo de alta velocidad con velocidades radiales entre 700 y 1100 km s^{-1} y otro grupo de baja velocidad que muestra velocidades por debajo de $\sim$250 km s^{-1}. Interpretamos que los nudos de alta velocidad pertencen al material eyectado por la explosión, y que los de baja velocidad es material chocado del medio circunestelar (CSM) formado en la pérdida de masa de pre-supernova. Las abundancias químicas de ambas poblaciones también muestran marcadas diferencias. El grupo de alta velocidad incluye un número substancial de nudos con significativamente altos cocientes de [N II]/Hα que no se ven en la población de baja velocidad, lo que sugiere un enriquecimiento mayor de nitrógeno en el material eyectado que en el CSM. Estos resultados son comparados con la evidencia de pérdida de masa de pre-supernova en la nebulosa del Cangrejo, quizás el remanente más similar a 3C 58. Estos remanentes pueden ser dos casos de estudio de pérdidas de masa de pre-supernova en progenitores de núcleos colapsantes de baja masa ($\sim 8 - 10\ M_\odot$).

ABSTRACT

We discuss the findings of a comprehensive imaging and spectroscopic survey of the optical emission associated with the supernova remnant 3C 58 (Fesen et al. 2007) as they relate to the topic of pre-SN mass loss. Spectroscopically measured radial velocities of over 450 emission knots within the remnant show two distinct kinematic populations of optical knots: a high-velocity group with radial velocities in the range of 700 – 1100 km s^{-1} and a lower velocity group exhibiting radial expansion velocities below $\sim$250 km s^{-1}. We interpret the high-velocity knots as ejecta from the SN explosion and the low-velocity knots as shocked circumstellar material (CSM) likely resulting from pre-SN mass loss. The chemical signatures of the two populations also show marked differences. The high velocity group includes a substantial number of knots with notably higher [N II]/Hα ratios not seen in the lower velocity population, suggesting greater nitrogen enrichment in the ejecta than in the CSM. These results are compared with evidence for pre-SN mass loss in the Crab Nebula, perhaps the remnant most similar to 3C 58. These SNRs may comprise two case studies of pre-SN mass loss in relatively low mass ($\sim 8 - 10\ M_\odot$) core-collapse progenitors.

Key Words: **CIRCUMSTELLAR MATTER — ISM: INDIVIDUAL (3C 58, CRAB NEBULA) — ISM: SUPERNOVA REMNANTS**

1. INTRODUCTION

3C 58 is a Galactic supernova remnant (SNR) with many similar properties to the Crab Nebula. Both remnants have rapidly spinning neutron stars (pulsars) which strongly influence their radio and X-ray morphologies. 'Crab-like' or 'plerionic' (filled-center) remnants, like 3C 58, are brightest toward their centers in both X-rays and in the radio (Weiler & Seielstad 1971; Wilson & Weiler 1976). The bright central emission in plerions is a result of the interaction between strong magnetic fields and the outflow of relativistic particles from the neutron star. This interaction produces the synchrotron emission seen in the resulting pulsar wind nebulae (PWN).

Aside from their classification as plerionic remnants, 3C 58 and the Crab share a number of other properties. Both are thought to have progenitors in the initial main sequence mass range of 8 – 10 $M_\odot$ (Nomoto et al. 1982; Nomoto 1985, 1987; Fesen 1983). Both remnants are also believed to be relatively young, with the Crab being the well established remnant of the historic guest star of 1054, while 3C 58 is proposed to be the SNR of a guest star seen in 1181 (Stephenson 1971; Clark & Stehenson 1997; Stephenson & Green 2002). The two remnants

[1]Physics & Astronomy Department, 6127 Wilder Laboratory, Dartmouth College, Hanover, NH 03755, USA (rudie@dartmouth.edu, fesen@snr.dartmouth.edu).

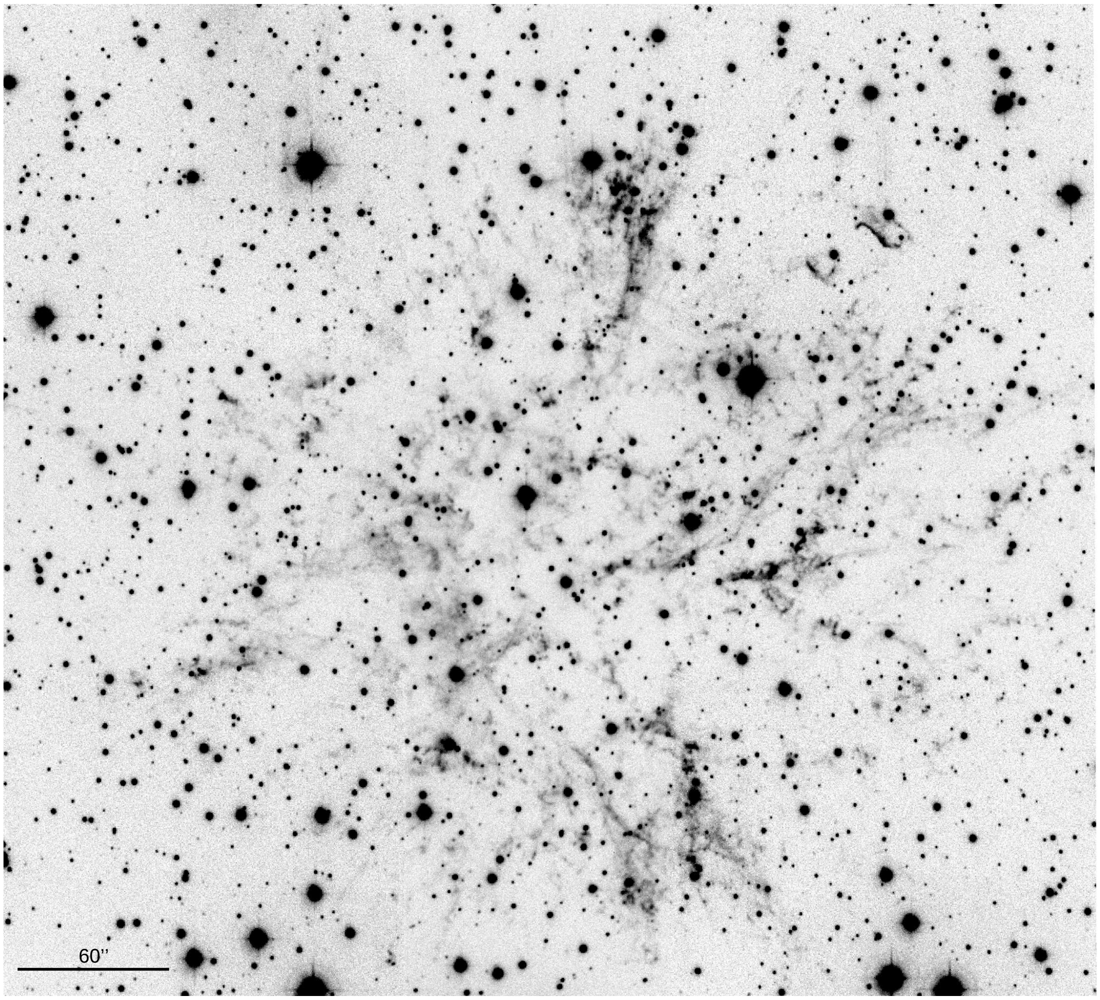

Fig. 1. A deep Hα image of the central regions of the 3C 58 supernova remnant (Fesen et al. 2007).

also exhibit similar expansion velocities: 3C 58 and the Crab have maximum V_R of 1100 km s^{-1} and 2200 km s^{-1} (Clark et al. 1983; Fesen & Ketelsen 1985; Lawrence et al. 1995) respectively. Such expansion velocities are comparatively low for young SNRs, implying a much lower kinetic energy of approximately $10^{49.5}$ erg compared with the canonical 10^{51} erg.

However, despite their similar expansion velocities and possibly similar ages, the remnants are quite different in physical size. The Crab nebula is located at a distance of $\sim$2 kpc (Davidson & Fesen 1985) and has an angular size of roughly $5' \times 7'$ (Wilson 1972) making it 3×4 pc in size. 3C 58 is farther away at $\sim$3 kpc (Green & Gull 1982; Roberts et al. 1993) and roughly $6' \times 10'$ (see Figure 1) (Wilson & Weiler 1976; Reynolds & Aller 1988), making it 5×9 pc or around twice the size of the Crab.

2. EVIDENCE FOR PROGENITOR MASS LOSS IN 3C 58

In a recent comprehensive spectral survey of 3C 58 completed by Fesen et al. (2007), radial velocities and compositions of 463 emission knots within the remnant were measured. The observed radial velocities in 3C 58 range from -1070 km s^{-1} to $+1100$ km s^{-1} and separate into two kinematically distinct velocity groups as shown in Figure 2. The high velocity group centers around 770 km s^{-1} and forms a thick shell with a velocity dispersion of ±155 km s^{-1}. The second group consists of much lower velocity emission knots. Measured radial velocities for this group range between -250 km s^{-1} and $+200$ km s^{-1}. There is a clear separation between these populations which only merge at radial distances from the pulsar of $\sim100''$. Both groups of

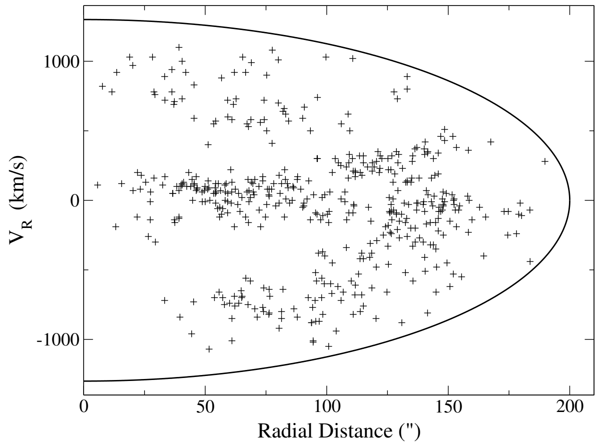

Fig. 2. Plot of observed knot radial velocity with projected knot radial distance from the remnant's central X-ray point source (PSR J0205+6449). The curve in the figure represents a spherical expansion of 1300 km s^{-1}.

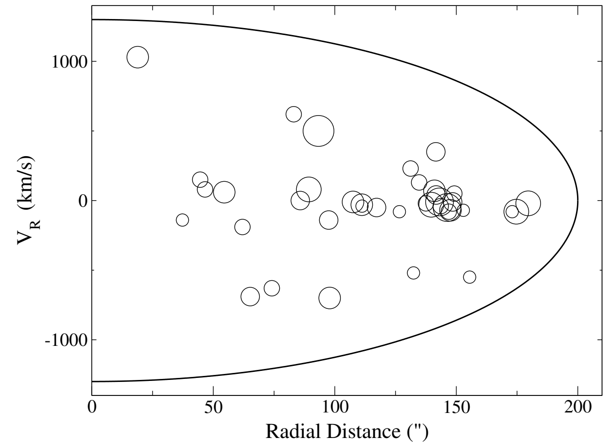

Fig. 3. Radial velocity of knots in 3C 58 with Hα flux $\geq 1 \times 10^{-15}$ erg cm^{-2} s^{-1}. Symbol size is proportional to the measured [S II] 6716/6731 line ratio; hence, the smaller symbol size indicates higher knot electron density.

emission knots are well distributed spatially across the remnant.

We interpret the presence of these two distinct emission knot populations as evidence for both SN ejecta and circumstellar material (CSM) within the 3C 58 remnant. The higher radial velocity knots are likely the ejecta from the SN explosion itself, while the slower ones may be shocked CSM. We believe the CSM knots to be the result of a pre-SN mass loss phase during which material from the progenitor star was ejected with velocities of ≤ 200 km s^{-1}. The low-velocity population of suspected CSM emission knots is substantial, making up approximately half of the optically emitting material near the remnant's center. The lack of any intermediate velocity knots within the remnant (see Figure 2) suggest the remnant's high-velocity ejecta is largely confined to an outer shell.

The distribution of knot density in 3C 58 is compared to radial velocity in Figure 3. Because the [S II] emission measurements from the fainter knots have significant errors, the plot only reflects the ratios of the brightest of 3C 58's knots. In this figure, the circle size corresponds to the [S II] 6716/6731 line ratio which is a density sensitive ratio. Higher [S II] 6716/6731 line ratios (larger circles) are representative of lower densities. The two velocity populations show no correlation to any sort of density pattern within the remnant.

In terms of composition, the two kinematic populations of emission knots differ noticeably. Since the [N II] 6548,6583 lines are not major nebular coolants, the observed [N II]/Hα ratio can be used as a first order indicator of relative N/H abundances. Within the high-velocity group, there is a substantial number of knots which show relatively high [N II]/Hα ratios. This trend is shown in Figure 4 which plots the correlation between the velocity pattern seen in the remnant and the composition of these two velocity groups. The circle size in this figure represents the observed [N II]/Hα line ratio. Knots with intermediate and low [N II]/Hα ratios are found in both the high and low velocity populations. However, knots showing relatively high [N II]/Hα ratios (i.e., the larger circles) are confined to the high-velocity knot population.

Interestingly, the highest [N II]/Hα knots lie toward the middle or inner edge of the maximum velocity range while the highest velocity knots show values closer to the average [N II]/Hα ratio. We would expect the highest velocity ejecta to originate from the surface of the star (thus having a composition similar to the CSM) while somewhat slower SN ejecta would have come from deeper within the star and therefore might exhibit a greater degree of nitrogen enrichment. This is the basic structure of the composition pattern observed within 3C 58. Thus, the composition measurements from the remnant support the scenario in which the low-velocity material is circumstellar mass loss ejected by the progenitor prior to the SN event, while the high-velocity material represents SN ejecta.

In general, the measured chemical abundances of the emission knots within the remnant support the notion of pre-SN mass loss. 3C 58 commonly ex-

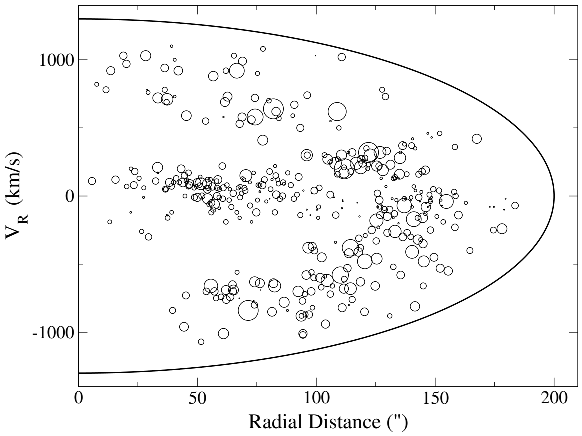

Fig. 4. Radial velocity of knots in 3C 58. Symbol size is proportional to the measured [N II]/Hα line ratio.

hibits strong [N II] emission ([N II]/H$\alpha \simeq 3 - 10$) which is considerably higher than ratios seen in shocked gas with solar composition (Cox & Raymond 1985; Hartigan et al. 1994). These ratio values suggest nitrogen enrichment at least several times solar (MacAlpine et al. 1996; Zanin & Kerber 2000), likely caused by CNO processing within the progenitor star. Similar [N II] line emission ratios have been observed in mass loss material found in Wolf-Rayet nebulae such as NGC 6888 (Kwitter 1981) and in young SNRs such as the QSFs in Cas A (van den Bergh 1971; Peimbert & van den Bergh 1971; Fesen 2001). This supports the conclusion that the low-velocity population is nitrogen-enriched stellar material shed by the progenitor before the SN event which has since been shocked by the expanding SNR.

3. SIMILARITIES BETWEEN 3C 58 AND THE CRAB NEBULA

In terms of its radio and X-ray emission, 3C 58 has long been viewed as a remnant with properties most similar to those of the Crab Nebula. However, it appears now that the 3C 58 and Crab Nebula remnants may have an added similarity, as both remnants show evidence for pre-SN mass loss.

The chief arguments in favor of CSM in the Crab Nebula lie in the chemical signature of an east-west band of He–rich filaments that circle the center of the remnant (MacAlpine et al. 1989), and the synchrotron 'bays' on the eastern and western edges of these filaments (Fesen et al. 1992). Additional evidence comes from several outlying filaments in the Crab which emit strong [N II] emissions compared to Hα (Fesen & Kirshner 1982; MacAlpine et al. 1996), not unlike that seen in the CSM knots in 3C 58.

On the other hand, the distribution of pre-SN mass loss material in the two remnants appears to be dissimilar. In 3C 58, the low-velocity CSM knots are uniformly distributed across the remnant. In contrast, within the Crab Nebula the circumstellar material was likely confined to a toroidal disk. The remnant of this disk is observed today as a helium–rich strip running east to west across the remnant (Uomoto & MacAlpine 1987) which exhibits a He I $\lambda 5876/H\beta$ line ratio > 0.9 compared to ratios as low as 0.38 away from this region near the base of the northern filamentary jet (MacAlpine et al. 1989).

Drift scans of the Crab nebula, in which the slit is oriented N-S, show a strong asymmetric N–S velocity pattern. That is, around the high-He band location, radial velocities are significantly lower than in the rest of the remnant. The overall velocity structure of the remnant resembles a figure eight or an hourglass, with the north and south regions exhibiting bubble-like bipolar structures. This bipolar expansion pattern might have been caused by SN ejecta confinement and deceleration by a toroidal disk composed of the high-He filaments (MacAlpine et al. 1989; Fesen et al. 1997). Fabry-Perot imaging spectroscopy of the remnant support such a toroidal morphology of the high–He band (Lawrence et al. 1995).

The coincidence between this pinched velocity structure and high He filaments suggest the possibility of a pre-SN structure built up by mass loss from the progenitor star. The observed He enrichment of this structure may have come from CNO cycle processing of stellar material prior to its ejection (Fesen & Kirshner 1982; MacAlpine et al. 1989, 1996). Similarly, in 3C 58, the high [N II]/Hα ratios suggest that the slow moving velocity group is pre-SN mass loss material in which strong He emission lines are too weak to easily detect.

A confined explosion in the Crab Nebula caused by the presence of an east–west circumstellar disk might also help explain the presence of the remnant's synchrotron 'bays'; two indentations on the eastern and western edges of the remnant which contain little synchrotron emission (Fesen et al. 1992). Optical proper motion measurements of these bays show them to be moving outward at a somewhat slower expansion rate, consistent with the constrained velocities in this region reported by MacAlpine et al. (1989). Polarization studies of the region also show the edges of the bays have extremely coherent polarization vectors suggesting well organized magnetic field loops parallel to the edges of the bays.

In the pre-SN mass loss model, the Crab's synchrotron bays could be the result of the magnetic field of the pulsar wrapping around a red-giant or asymptotic giant branch pre-SN mass loss circumstellar disk, thus blocking the progress of the charged particles emitting the synchrotron radiation (Fesen et al. 1992). The remains of this circumstellar disk are the high-He band of filaments, and in this scenario, the magnetic torus is anchored to this band (Fesen et al. 1992; Smith 2003). Fesen et al. (1992) hypothesize the progenitor mass loss could have been induced by a binary companion which would help confine the CSM to a thin disk capable of surviving the SN explosion.

In the case of 3C 58, the pre-SN mass loss distribution appears to be quite different. There is a clear separation between the two velocity populations (see Figure 2) suggesting that pre-SN circumstellar mass loss material did not confine the SN expansion. If the ejecta in 3C 58 had been decelerated by CSM present at the time of explosion, we would expect the confinement to be uneven, leaving a full range of velocities with no real separation between the two populations. Further, the velocity pattern observed in 3C 58 does not support the presence of a circumstellar disk.

4. THE 3C 58 PROGENITOR

In view of the similarities between the Crab and 3C 58 as outlined above, it is likely that the progenitors of 3C 58 and the Crab were similar in nature. The Crab Nebula has been suggested to be the result of an electron capture SN (Nomoto 1987). In this model, the Crab progenitor evolved into a helium star (with an extended red-giant-like envelope) via mass loss. During this helium star phase, electron captures by ^{24}Mg and ^{20}Ne effectively reduce the Chandrasekhar mass of the core, causing the progenitor's O+Ne+Mg degenerate core to collapse. This would occur prior to oxygen burning within the core as the smaller mass of this star would be unable to reach the necessary core temperature (Nomoto 1984).

Electron capture SNe, which are thought to be the end stage of intermediate mass stars ($8-12$ $M_{\odot}$), are likely to have lower kinetic energies. Because these SNe collapse with timescales determined by the electron capture rate rather than dynamical timescales, they release less kinetic energy. Oxygen deflagration further acts to decelerate the collapse velocities (Nomoto 1987). Thus, the shock wave in these events is considerably weaker than in canonical iron core collapse events. If the 3C 58 SN was also an electron capture event this might help explain its relatively low expansion velocity.

As discussed during this conference, the discovery of the red supergiant (RSG) progenitor of SN 2003gd (Van Dyk, Li, & Filippenko 2003; Smartt et al. 2004; Hendry et al. 2005) suggests an empirical RSG – Type IIP SN connection. This also indicates that low mass ($\sim 8-10\ M_{\odot}$) RSG progenitors may lead to SNe IIP. While the progenitors of the Crab and 3C 58 are believed to have been in this mass range, it is unclear if these two relatively unusual remnants resulted from typical SN IIP explosions.

5. CONCLUSIONS

The kinematic and chemical properties of 3C 58's optical emission knots strongly suggest the existence of appreciable pre-SN circumstellar material within the remnant.

3C 58 and the Crab Nebula share many properties which may include the presence of pre-SN mass loss. Because of these similarities, and the intermediate mass of these remnant's progenitors, they likely represent the result of relatively low energy core-collapse SNe brought on by electron capture.

Finally, if 3C 58 is really associated with the 1181 guest star, it is younger, but physically larger and expanding more slowly than the Crab Nebula. Since the kinematics of the ejecta in 3C 58 show no deceleration by the CSM found within the remnant (shown by the lack of intermediate velocities), the slow expansion velocities which characterize this remnant are difficult to explain. A solution is simply to discard the remnant's proposed association with the 1181 event and assume 3C 58 is much older than 1000 yrs. Such a conclusion is supported by several recent studies of the remnant. The synchrotron expansion rate (Bietenholz 2006), current internal energy of the PWN (Chevalier 2004, 2005), pulsar spindown age (Murray et al. 2002), and the amount of mass swept up by the PWN (as measured in the X-ray) (Chevalier 2004, 2005) all suggest an age of a few thousand years.

REFERENCES

Bietenholz, M. F. 2006, ApJ, 645, 1180
Chevalier, R. A. 2004, Adv. Space Res., 33, 456
Chevalier, R. A. 2005, ApJ, 619, 839
Clark, D. H., Murdin, P., Wood, R., Gilmozzi, R., Danziger, J., & Furr, A. W. 1983, MNRAS, 204, 415
Clark, D. H., & Stephenson, F. R. 1977, The Historical Supernovae (New York: Pergamon Press)
Cox, D. P., & Raymond, J. C. 1985, ApJ, 298, 651
Davidson, K., & Fesen, R. A. 1985, ARA&A, 23, 119
Fesen, R. A. 1983, ApJ, 270, L53
__________. 2001, ApJS, 133, 161

Fesen, R. A., Hurford, A., Rudie, G. C., & Soto, A., 2007, ApJS, submitted
Fesen, R. A., & Ketelsen, D. A. 1985, in The Crab Nebula and Related Supernova Remnants, ed. M. C. Kafatos & R. B. C. Henry (Cambridge: Cambridge Univ. Press), 89
Fesen, R. A., & Kirshner, R. P. 1982, ApJ, 258, 1
Fesen, R. A., Martin, C. L., & Shull, J. M. 1992, ApJ, 399, 599
Fesen, R. A., Shull, J. M., & Hurford, A. P. 1997, AJ, 113, 354
Green, D. A., & Gull, S. F. 1982, Nature, 299, 606
Hartigan, P., Morse, J., & Raymond, J. 1994, ApJ, 436, 125
Hendry, M. A., et al. 2005, MNRAS, 359, 906
Kwitter, K. B. 1981, ApJ, 245, 154
Lawrence, S. S., MacAlpine, G. M., Uomoto, A., Woodgate, B. E., Brown, L. W., Oliversen, R. J., Lowenthal, J. D., & Liu, C. 1995, AJ, 109, 2635
MacAlpine, G. M. & Uomoto, A., ApJ, 102, 218
MacAlpine, G. M., McGaugh, S. S., Mazzarella, J. M., & Uomoto, A. 1989, ApJ, 342, 364
MacAlpine, G. M., Lawrence, S. S., Sears, R. L., Sosin, M. S., & Henry, R. B. C. 1996, ApJ, 463, 650
Murray, S. S., Slane, P. O., Seward, F. D., Ransom, S. M., & Gaensler, B. M. 2002, ApJ, 568, 226
Nomoto, K. 1984, ApJ, 277, 791
__________. 1985, in The Crab Nebula and Related Supernova Remnants, ed. M. C. Kafatos & R. B. C. Henry (Cambridge: Cambridge Univ. Press), 97
__________. 1987, in IAU Symp. 125, The Origin and Evolution of Neutron Stars, ed. D. J. Helfand & J.-H. Huang (Dordrecht: Reidel), 281
Nomoto, K., Sparks W. M., Fesen, R. A., Gull, T. R., Miyaji, S., & Sugimoto, D. 1982, Nature, 299, 803
Peimbert, M., & van den Bergh, S. 1971, ApJ, 167, 223
Reynolds, S. P., & Aller, H. D. 1988, ApJ, 327, 845
Roberts, D. A., Goss, W. M., Kalberla, P. M. W., Herbstmeier, U., & Schwarz, U. J. 1993, A&A, 274, 427
Smartt, S. J., Maund, J. R., Hendry, M. A., Tout, C. A., Gilmore, G. F., Mattila, S., & Benn, C. R., 2004, Science, 303, 499
Smith, N. 2003, MNRAS, 346, 885
Stephenson, F. R. 1971, QJRAS, 12, 10
Stephenson, F. R., & Green, D. A. 2002, Historical Supernovae and Their Remnants (Oxford: Clarendon Press)
Uomoto, A. & MacAlpine G. M. 1987, ApJ, 96, 1511
van den Bergh, S. 1978, ApJ, 165, L457
Van Dyk, S. D., Li, W., & Filippenko, A. V. 2003, PASP, 115, 1289
Weiler, K. W., & Seielstad, G. A. 1971, ApJ, 163, 455
Wilson, A. S. 1972, MNRAS, 157, 229
Wilson, A. S., & Weiler, K. W. 1976, A&A, 49, 357
Zanin, C., & Kerber, F. 2000, A&A, 356, 274